© 2016. Published by The Company of Biologists Ltd | Journal of Cell Science (2016) 129, 1500-1511 doi:10.1242/jcs.185199

RESEARCH ARTICLE

Post-transcriptional regulation mediated by specific neurofilament introns *in vivo*

Chen Wang and Ben G. Szaro*

ABSTRACT

Neurons regulate genes post-transcriptionally to coordinate the supply of cytoskeletal proteins, such as the medium neurofilament (NEFM), with demand for structural materials in response to extracellular cues encountered by developing axons. By using a method for evaluating functionality of cis-regulatory gene elements *in vivo* through plasmid injection into *Xenopus* embryos, we discovered that splicing of a specific *nefm* intron was required for robust transgene expression, regardless of promoter or cell type. Transgenes utilizing the *nefm* 3′-UTR but substituting other *nefm* introns expressed little or no protein owing to defects in handling of the messenger (m)RNA as opposed to transcription or splicing. Post-transcriptional events at multiple steps, but mainly during nucleocytoplasmic export, contributed to these varied levels of protein expression. An intron of the β-globin gene was also able to promote expression in a manner identical to that of the *nefm* intron, implying a more general preference for certain introns in controlling *nefm* expression. These results expand our knowledge of intron-mediated gene expression to encompass neurofilaments, indicating an additional layer of complexity in the control of a cytoskeletal gene needed for developing and maintaining healthy axons.

KEY WORDS: Post-transcriptional regulation, Cis-regulatory elements, Intron, Neurofilament, *Xenopus laevis*

INTRODUCTION

Axon outgrowth during nervous system development requires the coordinated synthesis of multiple neuronal cytoskeletal proteins. This coordinated synthesis is an ongoing dynamic process involving changes in gene expression that are tightly regulated at both the transcriptional and post-transcriptional levels in response to spatial and temporal cues (reviewed in Szaro and Strong, 2011). Because their subunit composition changes continually with each stage of axon development, the neurofilaments provide a prime example of this regulation. As the intermediate filaments of neurons and the most abundant cytoskeletal polymer of vertebrate myelinated axons, neurofilaments contribute to the formation, consolidation and maintenance of the overall neuronal cytoskeletal network. Properly regulated neurofilament gene expression promotes axon outgrowth and controls axon caliber, whereas dysregulated expression contributes to the pathogenesis of neurodegenerative disease (reviewed in Szaro and Strong, 2010; Thyagarajan et al., 2007).

In both rodents and *Xenopus*, expression of the three type IV neurofilament triplet subunit proteins [i.e. light (NEFL), medium (NEFM), and heavy (NEFH) neurofilament proteins] responds to cues encountered by growing axons (Schwartz et al., 1990; Undamatla and Szaro, 2001; Zhao and Szaro, 1995). For example, during developmental and regenerative axon outgrowth, increased expression that is stimulated by axons making appropriate contacts is principally due to dynamic changes in nucleocytoplasmic export, stability, and translation of neurofilament RNAs, as opposed to changes in gene transcription (Ananthakrishnan et al., 2008; Ananthakrishnan and Szaro, 2009; Schwartz et al., 1994). In mature neurons, post-transcriptional changes in neurofilament messenger (m)RNA metabolism also contribute significantly to neurodegeneration (Cañete-Soler et al., 1999; Ge et al., 2003; Nie et al., 2002). To date, studies of the molecular mechanisms responsible for these post-transcriptional changes have focused mainly on identifying trans-factors [e.g. RNA-binding proteins and micro (mi)RNAs] that bind to neurofilament RNAs. At least three of the proteins that bind to neurofilament mRNAs – hnRNP K (Thyagarajan and Szaro, 2004, 2008), TDP-43 (Strong et al., 2007) and FUS/TLS (Lagier-Tourenne et al., 2012) – have important functions in development and disease. For example, regulation of neurofilament and other cytoskeletal-related mRNAs by hnRNP K is specifically required for axon outgrowth (Liu et al., 2008; Liu and Szaro, 2011), and all three RNA-binding proteins have been implicated more generally in motor neuron disease (Arai et al., 2006; Kwiatkowski et al., 2009; Lagier-Tourenne and Cleveland, 2009; Moujalled et al., 2015). These proteins bind not only to the 3′ untranslated regions (UTRs) of their target RNAs but also to the introns of a variety of neuronal pre-mRNAs (Cao et al., 2012; Lagier-Tourenne et al., 2012), suggesting that these proteins influence multiple phases of the lives of their targeted RNAs, and that their associations with introns could themselves be coupled with subsequent events in the trafficking and translation of the mRNAs (Lagier-Tourenne et al., 2012). Introns are well known to influence gene expression at multiple levels (Le Hir et al., 2003), but what role intron splicing plays for neurofilament RNAs is unknown, especially within the context of the natural regulation of neurofilament gene expression that takes place within an intact developing vertebrate nervous system. Answering this question is important for our understanding of the regulation of neuronal cytoskeletal composition in development and also has broader implications for neurodegenerative diseases.

Our recently developed *in vivo* technique for testing the activity of cis-regulatory gene regions in F_0 generation *Xenopus laevis*, by injecting plasmids expressing fluorescent reporter genes into two-cell-stage embryos (Wang and Szaro, 2015), provides an ideal experimental system for addressing the role of introns in neurofilament gene expression in an intact developing vertebrate. Of the neurofilament triplet genes, we chose to analyze the *nefm* gene, because its early expression in neural development (Bennett et al., 1988; Carden et al., 1987; Szaro et al., 1989), two-intron gene structure (Roosa et al., 2000) and 3′-UTR sequences (Thyagarajan

Department of Biological Sciences and the Center for Neuroscience Research, University at Albany, State University of New York, 1400 Washington Avenue, Albany, NY 12222, USA.

*Author for correspondence (bgs86@albany.edu)

Received 18 December 2015; Accepted 17 February 2016

Journal of Cell Science

Journal of Cell Science (2016) 129, 1500-1511 doi:10.1242/jcs.185199

and Szaro, 2004) are phylogenetically highly conserved from *Xenopus* to mammals. We discovered that the nature of the intron itself, as well as splicing, is crucial for subsequent post-transcriptional events that culminate in protein expression. Our findings demonstrate the existence of an additional layer of complexity in the control of cytoskeletal composition, which neurons use to grow and maintain a healthy axon.

RESULTS

The second intron of the *nefm* gene promotes reporter protein expression *in vivo*

To study the activity of cis-regulatory gene elements controlling post-transcriptional regulation of the *nefm* RNA within the biological context of a developing nervous system, we injected plasmids bearing different cis-elements into *Xenopus laevis* embryos (Wang and Szaro, 2015). In this method, plasmids containing an *attB* element and two insulator sequences flanking the reporter gene are injected into two-cell-stage embryos to yield promoter-specific reporter expression in F_0 generation tadpoles that persists through at least early tadpole stages, thereby obviating the need to create transgenic lines. Two fluorescent reporter constructs, a 'test' and a 'reference' plasmid, are co-injected unilaterally into the embryos (Fig. 1). The test construct expresses a red fluorescent protein (DsRed2) and contains the cis-regulatory regions of interest, whereas the reference plasmid expresses a green fluorescent protein (glGFP) to serve both as a control for selecting successfully injected embryos and as a normalization factor in subsequent biochemical analyses. In the current study, injected embryos were raised to late tailbud stages (stages 43–44), by which time they are completely transparent, and *Xenopus nefm* exhibits a mature expression pattern (Szaro et al., 1989; Szaro and Gainer, 1988; Undamatla and Szaro, 2001).

We initially set out to identify post-transcriptional cis-regulatory elements of the *nefm* gene by analyzing the *in vivo* activity of its 3′-UTR, because this region of the gene is highly conserved phylogenetically, contains multiple predicted binding sites for miRNAs, and binds to several RNA-binding proteins that post-transcriptionally regulate *nefm* expression (Liu et al., 2008; Thyagarajan and Szaro, 2004, 2008). For the reference plasmid, *glGFP* was flanked by a 1.5 kb *nefm* promoter and a rabbit β-globin (*hbb2*) 3′-UTR, which have been demonstrated previously to yield robust reporter protein expression in neurons by stages 43–44 (Wang and Szaro, 2015). For the test plasmid, the *hbb2* 3′-UTR and *glGFP* were replaced with the *Xenopus nefm* 3′-UTR and *DsRed2*, respectively (Fig. S1). When co-injected, the reference plasmid gave strong glGFP expression, confirming that procedures had been performed successfully, but the test plasmid generated very little protein (Fig. 2A, intronless), indicating that the *nefm* 3′-UTR needed additional elements for optimal *in vivo* activity. Such elements might lie anywhere upstream of the 3′-UTR, but because introns are well known to enhance expression of reporter genes (Buchman and Berg, 1988; Callis et al., 1987; Duncker et al., 1997; Hamer et al., 1979; Le Hir et al., 2003; Palmiter et al., 1991), we opted to test *nefm* introns first.

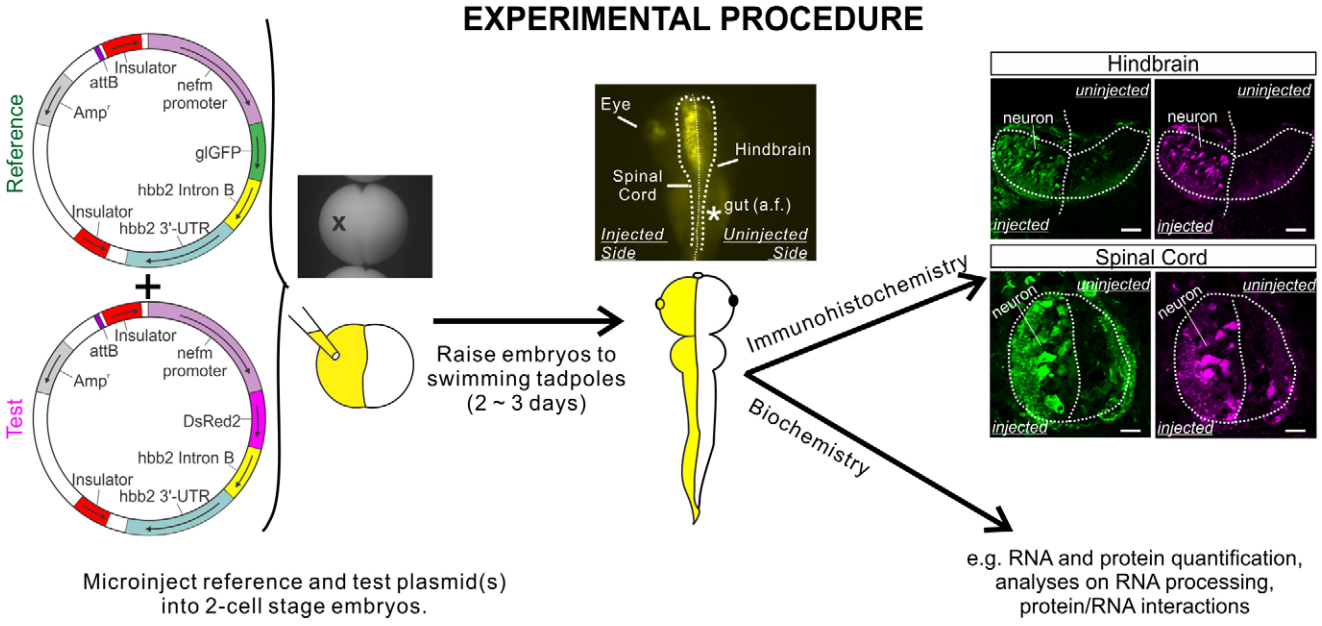

Fig. 1. Microinjection of specialized plasmid DNAs into *Xenopus* embryos to analyze cis-regulatory gene element activity *in vivo* by using immunohistochemical and biochemical methods. (Left) A glGFP-expressing reference (top) was co-injected unilaterally into two-cell-stage embryos, together with various DsRed2-expressing test plasmids (e.g. bottom) bearing cis-elements of interest. Reference plasmid expression served as an internal control for the injection procedure, and as a normalizing factor for analyzing test plasmid RNA and protein expression. Both plasmids possessed special elements (*attB* and insulator sequences) for facilitating persistent promoter-specific expression in F_0 animals (Wang and Szaro, 2015). For the purpose of demonstrating the use of the method, both plasmids shown here are driven by an *nefm* promoter, restricting reporter expression to neuronal tissues. X indicates the injection site on a two-cell-stage embryo. (Middle) By stages 43–44 (late tailbud stages), tissue-specific expression of reporter proteins in cells that had descended from the injected blastomere (left side of all images) could be visualized in live embryos through a fluorescence stereo microscope. (Middle, top) Representative example of the anterior of a stage 43–44 embryo, previously co-injected with a *glGFP* reference plasmid and a *DsRed2* test plasmid containing identical cis-regulatory elements, under the control of a neuronal promoter (taken with a Nikon DS-Ri1 camera). *a.f., autofluorescence in the developing gut. (Right) Embryos exhibiting appropriate expression of the reference plasmid were selected for further analyses of expression with double-label immunohistochemistry (green, glGFP; magenta, DsRed2) of cryosections through hindbrain and spinal cord (right, top) and by biochemical analyses of whole embryos (right, bottom). Immunostained transverse cryosections were imaged with a Zeiss LSM 510 confocal laser-scanning microscope. Dots outline the central nervous system, and the vertical dotted lines separate the injected (left) and uninjected sides. Scale bars: 20 µm (hindbrain); 50 µm (spinal cord).

Journal of Cell Science (2016) 129, 1500-1511 doi:10.1242/jcs.185199

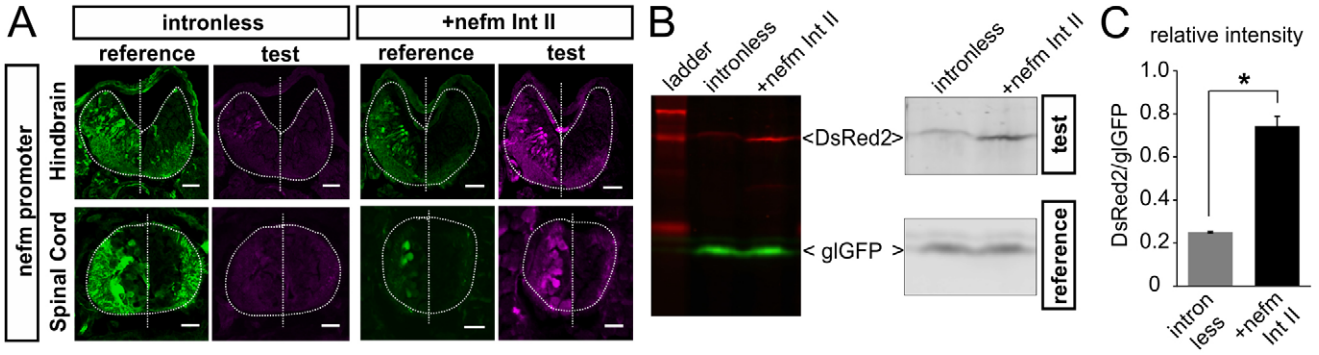

Fig. 2. Reporter genes driven by the *nefm* promoter and paired with the *nefm* 3′-UTR yielded markedly stronger protein expression when the test plasmid contained the second intron of *nefm* (+nefm Int II) than when it was intronless. Embryos were injected with the indicated DsRed2-expressing test plasmid simultaneously with the glGFP reference plasmid (as in Fig. 1) and raised to stage 43–44 for analysis. (A) Double-label immunohistochemistry for glGFP (green) and DsRed2 (magenta) of representative sections from hindbrain and spinal cord (40–50 sections from three animals each, for this and all subsequent figures). Although both groups exhibited strong glGFP expression from the reference plasmid, only those receiving the *nefm* Intron II test construct expressed DsRed2 strongly. Dotted lines outline the central nervous system. Vertical dotted lines separate the injected and uninjected sides. Scale bars: 20 µm (hindbrain); 50 µm (spinal cord). (B) Color: native fluorescence of DsRed2 (top band; test) and glGFP (bottom band; reference) from whole-embryo extracts, separated and visualized directly on full-length partially denaturing SDS 12% polyacrylamide gels (fluorescent SDS PAGE) to confirm differences in fluorescent reporter expression. DsRed2 runs as a dimer at ~54 kDa and glGFP as a monomer at ~27 kDa. Ladder: marker proteins running at ~65, 50 and 30 kDa. Monochrome: images representative of those used for quantification showing DsRed2 and glGFP bands. (C) Relative intensities of the DsRed2 fluorescent bands (normalized to glGFP fluorescence in the same lane) from the two groups further confirmed that expression was significantly greater for embryos expressing reporter genes containing *nefm* Intron II than those expressing the intronless counterparts. **P*<0.01, Student's *t*-test; *n*=3 replicates of 30 pooled embryos for each condition; error bars, s.e.m.

To test whether an upstream *nefm* intron would promote protein expression, we created new test plasmids by placing the last intron (Intron II) of *Xenopus nefm* near to the 3′ end of the DsRed2-coding sequence (Fig. S1), upstream of the stop codon and *nefm* 3′-UTR to protect against nonsense-mediated decay (reviewed in Sun and Maquat, 2000). As determined by immunohistochemistical analysis of hindbrain and spinal cord, and by quantifying fluorescence in whole-embryo extracts on partially denaturing SDS 12% polyacrylamide gels (fluorescent SDS PAGE), addition of this intron boosted protein expression by approximately threefold over that of the intronless construct (Fig. 2A–C). To test whether these effects were specific to Intron II, we replaced it with the only other intron in *nefm*, Intron I (Fig. S1). Protein expression with this construct, however, was virtually undetectable (Fig. 3A,D,E; >14-fold less than Intron II), despite the intron having been successfully spliced from expressed transcript (as determined by cloning and sequencing of the RNAs extracted directly from injected embryos). Thus, although *nefm* has two introns, only the splicing of Intron II yielded optimal reporter protein expression.

Splicing alone is necessary but not sufficient for expression

To test whether splicing of Intron II alone is sufficient to produce the observed enhanced expression or whether the presence of additional elements within this intron were also needed, we constructed two more test plasmids (Fig. S1). The first had a minimal spliceable *nefm* Intron II, comprising 105 and 120 nucleotides from the 5′ and 3′ ends, respectively, of the original full-length Intron II construct. Cloning and sequencing of the expressed RNA from injected embryos confirmed that this intron was indeed spliced *in vivo* and that the resultant RNA sequences were identical to those produced from the full-length Intron II construct. The second plasmid used an unspliceable *nefm* Intron II, which lacked 11 bp and 21 bp from the 5′ and 3′ ends, respectively, of the full-length intron, eliminating the native splice sites and rendering the intron unspliceable. In all cases, the co-injected reference plasmid yielded glGFP expression as usual, whereas neither test variant yielded detectable DsRed2 protein (Fig. 3B–D). Quantification by performing fluorescent SDS PAGE indicated that the levels of DsRed2 protein from these two variants, whether spliced or unspliced, were more than 20-fold less than that generated with the full-length Intron II (Fig. 3E).

Variations in protein expression profiles associated with the introns are caused by differences in post-transcriptional regulation

To gain insights into which control points in gene expression, from transcription to translation, are affected by having various introns, we assayed levels of reporter RNAs from different intracellular pools. Using primers targeting the reporter-coding regions, we first measured the steady-state levels of reporter RNA from total cellular RNA, normalizing expression of *DsRed2* to that of *glGFP* and expressing results as a percentage of the expression of the intronless construct group (Fig. 4A). The construct with the full-length Intron II generated the most reporter RNA, approximately threefold more than the intronless group, which corresponded well with the threefold increase seen in protein expression (Fig. 2C). Thus, the difference in protein expression between these two groups could be accounted for by a difference in the total amount of steady-state RNA. However, differences in total RNA expression between the other intron groups and the full-length Intron II group were too small to account for the much larger differences seen in protein expression. For example, the full-length Intron II construct yielded from ~14 to >20-fold more protein than did the Intron I, minimal spliceable Intron II and unspliceable Intron II constructs (Fig. 3D,E), whereas it produced only 3.1-, 1.4- and 9-fold higher steady-state levels of total RNA, respectively (Fig. 4A). These disparities between RNA and protein expression profiles suggested that additional regulatory mechanisms other than those that regulate steady-state levels of total RNA contribute to variations in protein expression seen among the introns.

To test whether variations in RNA expression from different introns were due to differences in transcription, we performed real-time quantitative PCR (RT-qPCR) analyses to quantify nascent unspliced transcript by using primers spanning the 3′ splice-site of the introns to yield amplicons of the same length that could only have been amplified from unspliced transcript. Quantification by performing RT-qPCR demonstrated that all four intron-containing

Journal of Cell Science (2016) 129, 1500-1511 doi:10.1242/jcs.185199

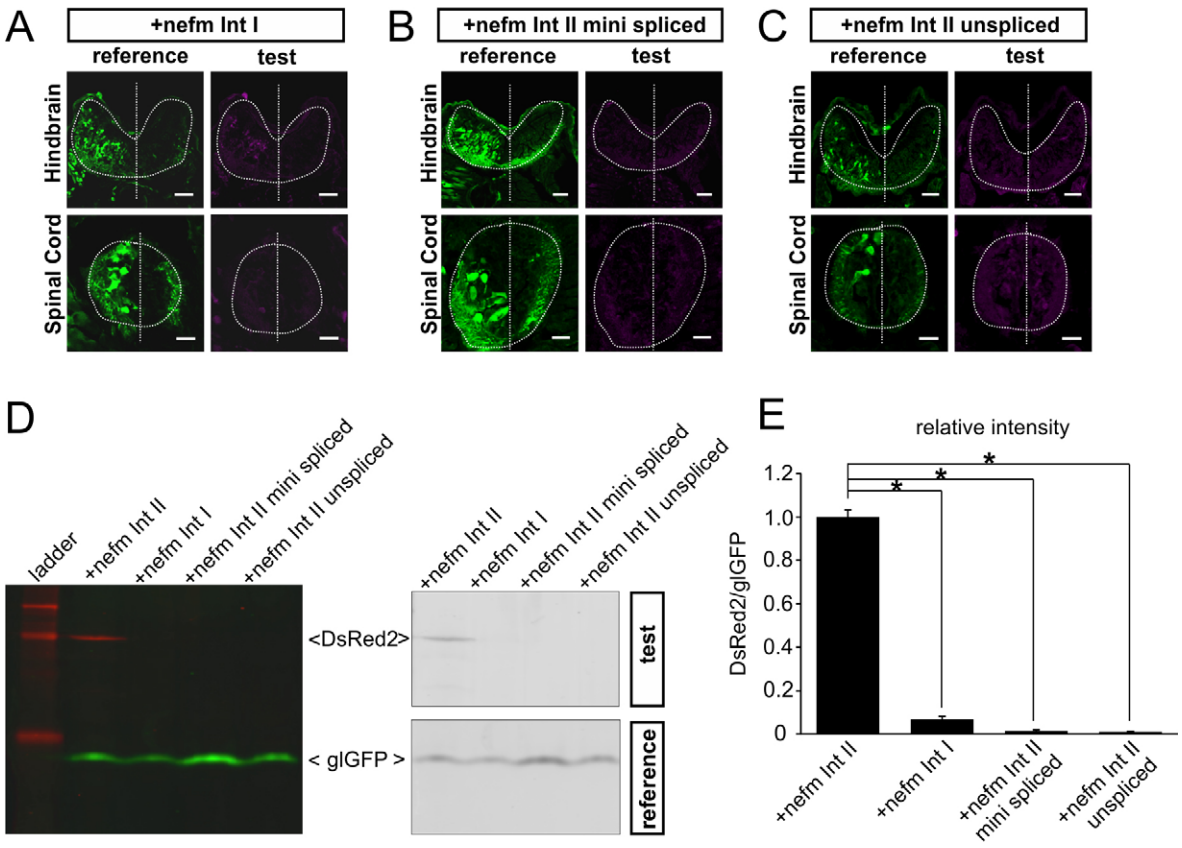

Fig. 3. Splicing was necessary, but not by itself sufficient, for robust protein expression of the *nefm* reporter gene. (A–C) Immunostained transverse cryosections of hindbrain and spinal cord of stage 43–44 embryos that had been co-injected with the same reference plasmid as described in Fig. 2 and a test plasmid bearing either (A) a full-length *nefm* Intron I (+nefm Int I), (B) a minimal spliceable *nefm* Intron II (+nefm Int II mini spliced) – which contained 98 bp and 100 bp from the 5′ and 3′ ends, respectively, of the original Intron II that had been used in the full-length Intron II construct, so that the spliced products derived from these constructs would be identical, and (C) an unspliceable *nefm* Intron II (+nefm Int II unspliced) – which contained Intron II but lacked 11 and 20 nucleotides from the 5′ and 3′ ends of the intron, respectively. Whereas robust glGFP expression of the reference plasmid on the injected side (left of each section) indicated that experimental procedures were successful for all groups, DsRed2 expression of the test plasmids was barely visible in the same sections. Dotted lines outline the central nervous system. Vertical dotted lines separate the injected and uninjected sides. Scale bars: 20 µm (hindbrain); 50 µm (spinal cord). (D) Fluorescent SDS PAGE and (E) quantification of relative fluorescence intensities, which were performed, analyzed, and annotated as described in Fig. 2, confirmed that the full-length Intron II yielded significantly more DsRed2 expression than did Intron I and the two Intron II variants. **P*<0.01 (Student's *t*-test); *n*=3 replicates of 30 pooled embryos for each condition; error bars, s.e.m.

groups generated equivalent amounts of nascent unspliced RNA (Fig. 4B), despite their having yielded widely varying levels of both protein and total RNA. Thus, the differences in steady-state levels of reporter RNA among the four intron-containing groups arose not from differences in transcription, but rather from subsequent differences in RNA processing. Because such processing takes into account the combined effects of pre-mRNA splicing and stability on mRNA levels, these differences were more readily and directly compared by encapsulating them into a single new statistic, termed mRNA processing efficiency (Fig. 4C). This statistic was calculated by subtracting the ratio of nascent to total RNA from 100%. As expected from the higher total RNA levels, the mRNA processing efficiency was modestly but nonetheless significantly greater (P<0.01; Student's t-test) for the full-length *nefm* Intron II group than for the other three intron groups (1.3, 1.1 and 3.0 times greater than the Intron I, minimal spliceable Intron II and unspliced Intron II groups, respectively). Thus, variations in the levels of reporter RNA among these intron groups arose primarily from differences in post-transcriptional rather than transcriptional control.

Although differences in post-transcriptional control among the four intron-containing groups were statistically significant, they were insufficient to account for the larger differences seen in protein expression. One possibility was that the transcripts produced remained trapped within the nucleus, making them unavailable for translation. To test this possibility, we compared the ratio of cytoplasmic to nuclear reporter mRNA levels (Fig. 4D). Consistent with other analyses, the full-length Intron II group exhibited the highest ratio, with ∼10.4 times more *DsRed2* mRNA in the cytoplasm than in the nucleus. In contrast, the Intron I and minimal spliced Intron II groups had less reporter RNA in the cytoplasm than in the nucleus (52% and 77%, respectively; Fig. 4D). Moreover, there was no detectable unspliced Intron II RNA in the cytoplasm (thus unplotted). Consequently, the efficiency of export from the nucleus of the full-length Intron II transcript was 20- and 14-fold greater than that of Intron I and the minimal spliced Intron II, respectively. From these data, we conclude that marked differences in nucleocytoplasmic export of transcripts among the four intron-bearing constructs are the main contributor to the differences in protein expression profiles seen in our system. In summary, accumulated differences in post-transcriptional regulation, arising from diverse ways of handling the transcripts, ultimately make the *nefm* Intron II an optimal intron for promoting protein expression when paired with the *nefm* 3′-UTR.

Journal of Cell Science (2016) 129, 1500-1511 doi:10.1242/jcs.185199

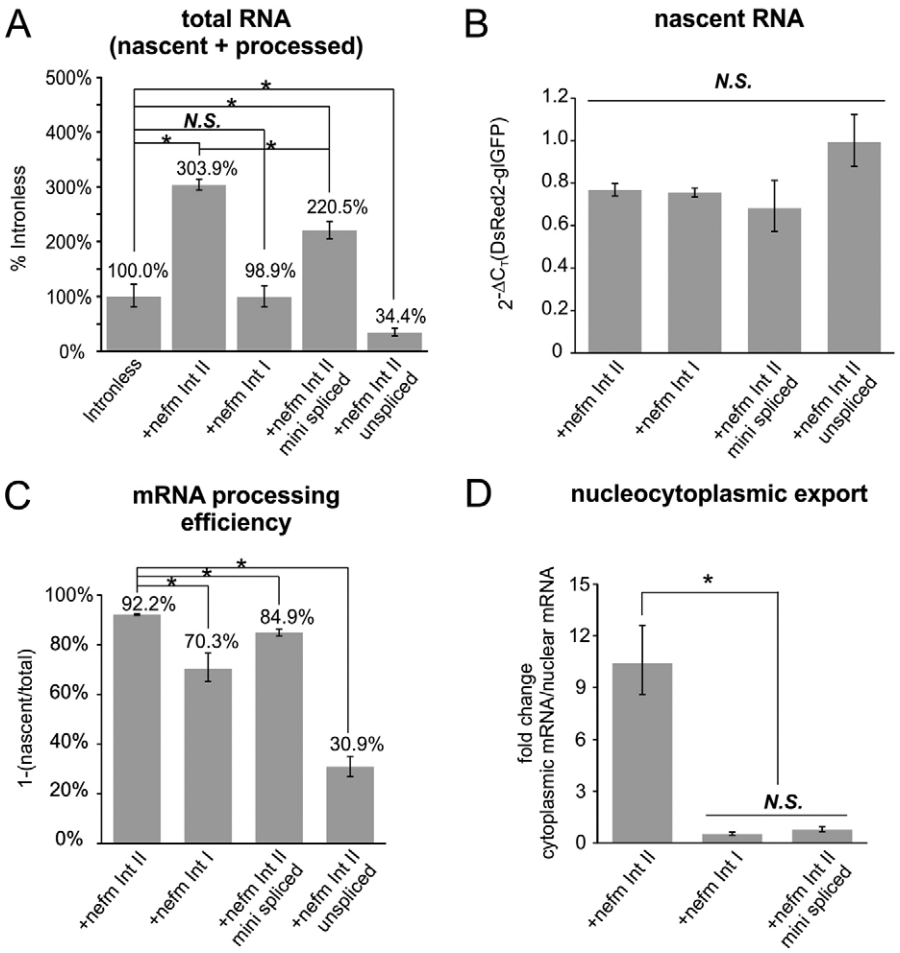

Fig. 4. Variations in protein expression among introns arose from differences in post-transcriptional regulation operating at multiple control points. (A–C) Total RNA was isolated from stage 43–44 embryos that had been previously co-injected with the *glGFP* reference plasmid and each of the indicated *DsRed2* test plasmids. (A) Significant variations in reporter RNA expression were seen across all constructs, except between the intronless and *nefm* Intron I (nefm Int I) constructs. Expression of *DsRed2* RNA relative to that of *glGFP* was determined by performing RT-qPCR (ΔC_T) for each replicate (n=3 from 30 pooled embryos) using primers targeting sequences within each coding sequence for each reporter. For presentation, ΔC_T was converted to a fold change ($2^{-\Delta C_T}$) and then expressed as a percentage of the value of the intronless group. (B) All intron-bearing constructs gave rise to equivalent amounts of nascent RNAs. Levels of nascent unspliced pre-mRNAs bearing the test reporter *DsRed2* were determined by performing RT-qPCR analysis, using the same cDNAs that are described in A as templates but with primers spanning 200 bp of the 3′ splice junctions. Forward primers targeted sites near to the 3′ end of each intron, and the reverse primer, which was the same for all constructs, targeted the downstream 3′-UTR. *DsRed2* nascent transcript levels are presented as a relative fold change over that of *glGFP* expression [$2^{-\Delta C_T(\text{DsRed2-glGFP})}$]. (C) mRNAs derived from Intron I and the two Intron II variants were subjected to less efficient post-transcriptional processing compared with full-length Intron II. Overall processing efficiencies of the mRNAs were evaluated by taking the ratio of nascent unspliced RNAs given in B to the total RNA obtained in A, converting this ratio to a percentage, and subtracting the result from 100%. (D) Nucleocytoplasmic export of RNAs expressed from Intron I and the mini spliceable Intron II constructs was significantly hindered compared with that of the full-length Intron II. RT-qPCR analysis was performed separately on total RNA isolated from nuclear and cytoplasmic subcellular fractions, using the same primers as used in A. ΔC_T (cytoplasmic–nuclear) for *DsRed2* was determined for each sample, averaged (mean±s.e.m.; n=3 biological replicates of ten embryos each), and converted to a fold change ($2^{-\Delta C_T}$; i.e. cytoplasmic/nuclear). (A–D) *P<0.02; N.S., P>0.05 (one-way ANOVA with Tukey's post-hoc tests). Error bars (s.e.m.) are asymmetric owing to the conversion from ΔC_T to $2^{-\Delta C_T}$ (fold change). [Note, mRNA processing and export of the *glGFP* reference RNA were analyzed in similar ways and showed no significant differences across the same groups (Fig. S2)].

nefm Intron II works independently of the promoter and tissue type to promote protein expression

We next tested the intronless construct and the full-length Intron II construct with different promoters to assess whether this intron required specific promoter elements and expression in neurons to function. For these tests, we replaced the *nefm* promoter with two new promoters – a neuronal β-tubulin promoter (*tubb2b*), which like the *nefm* promoter drives expression in neurons, and a cardiac actin promoter (*actc1*), which drives expression in muscle cells. For each new promoter, we created three plasmids: two DsRed2-expressing test plasmids (intronless and full-length *nefm* Intron II) both with the *nefm* 3′-UTR, and a glGFP-expressing reference plasmid with the original *hbb2* 3′-UTR (Fig. S1). With both new promoters, the *nefm* Intron II successfully promoted protein expression compared with its intronless counterpart – the *tubb2b* promoter in neurons (Fig. 5A) and the *atct1* promoter in muscle cells (Fig. 5D). Quantification by performing fluorescent SDS PAGE (Fig. 5B,C,E,F) further demonstrated that this increased expression was both statistically significant (P<0.01, Student's t-test) and comparable in magnitude to that seen with the *nefm* promoter (two- and fourfold greater for *tubb2b* and *atct1*, respectively, vs threefold for *nefm*). Thus, *nefm* Intron II promoted *in vivo* protein expression independently of both promoter and tissue type, further supporting the conclusion that effects on protein expression are mediated post-transcriptionally (see Discussion).

Journal of Cell Science (2016) 129, 1500-1511 doi:10.1242/jcs.185199

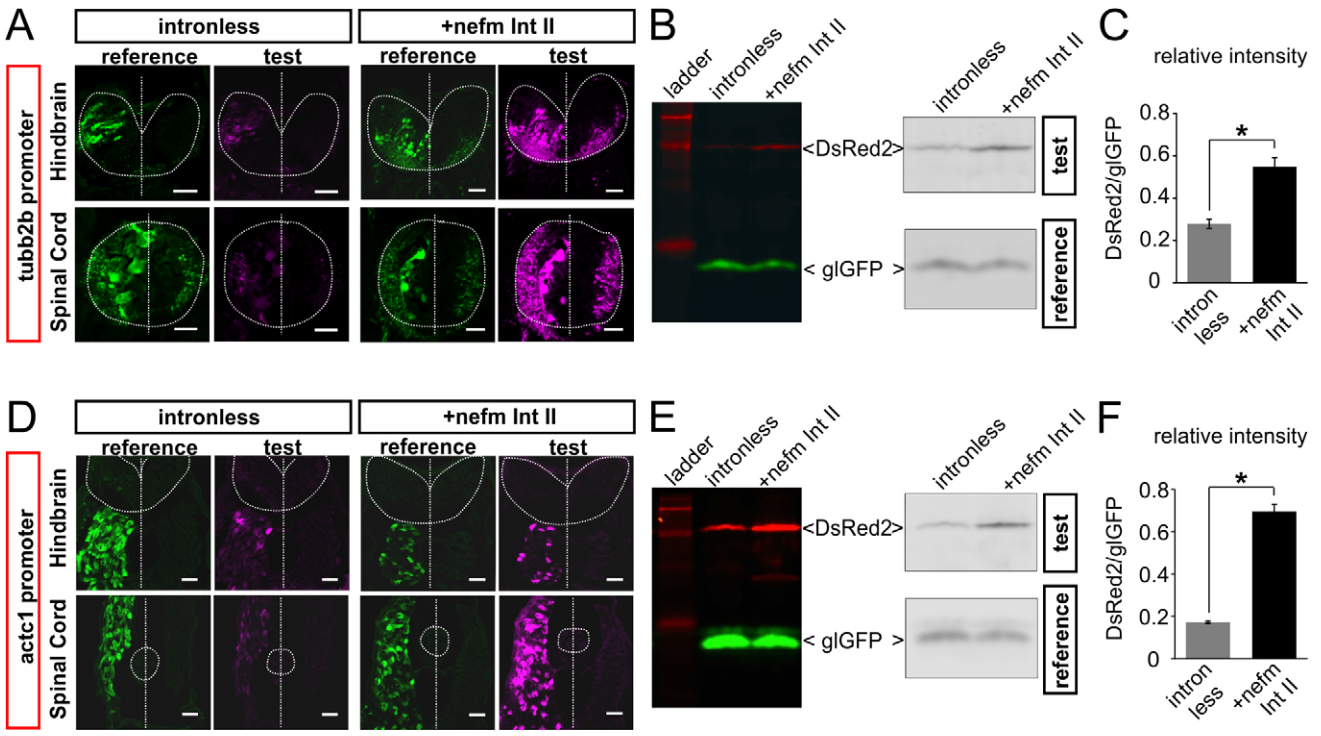

Fig. 5. *nefm* Intron II increased protein expression independently of promoter and tissue type. Embryos were injected with constructs bearing either no intron (intronless) or the *nefm* Intron II (+nefm Int II) driven by either a neuronal β-tubulin (*tubb2b*) promoter, which drives expression in the nervous system (A–C), or a cardiac actin (*actc1*) promoter, which drives expression in muscle cells (D–F). A reference glGFP-expressing plasmid bearing the same promoter (*tubb2b* or *actc1*) as its corresponding test plasmid was co-injected in each case. Procedures, analyses and annotations were otherwise the same as described for Fig. 2. Dotted lines outline the central nervous system. Vertical dotted lines separate the injected and uninjected sides. Scale bars: 20 µm (hindbrain); 50 µm (spinal cord). **P*<0.01 (Student's *t*-test); *n*=3 replicates of 30 pooled embryos for each condition; error bars, s.e.m.

The second intron of a rabbit β-globin gene and *nefm* Intron II promote equivalent expression

Our results raised the additional question of whether the introns and 3′-UTRs of other genes display properties similar to those of *nefm* Intron II with its 3′-UTR. Closer inspection of the *hbb2* 3′-UTR of the reference plasmid revealed that it in fact contained a ∼0.6-kb-long intron (*hbb2* Intron B), representing the second (and last) intron of the rabbit β-globin gene. In another context, the *hbb2* Intron B has been shown to promote both protein expression and nucleocytoplasmic mRNA export when included in a reporter construct transfected into BHK and COS cells (Rafiq et al., 1997). Thus, we were further motivated to test whether the *hbb2* Intron B would function in a similar way in our system. To test whether this intron has the same effect on protein expression of test plasmids containing the *hbb2* 3′-UTR, we deleted *hbb2* Intron B (Fig. S1) and found that protein expression diminished significantly, by approximately threefold from that of the intron-bearing construct (Fig. 6). This difference was equivalent to that seen when the *nefm* Intron II was deleted from the construct comprising the *nefm* 3′-UTR. Next, to test whether *hbb2* Intron B promotes protein expression when coupled with the *nefm* 3′-UTR, we replaced *nefm* Intron II with *hbb2* Intron B, while retaining the *nefm* 3′-UTR

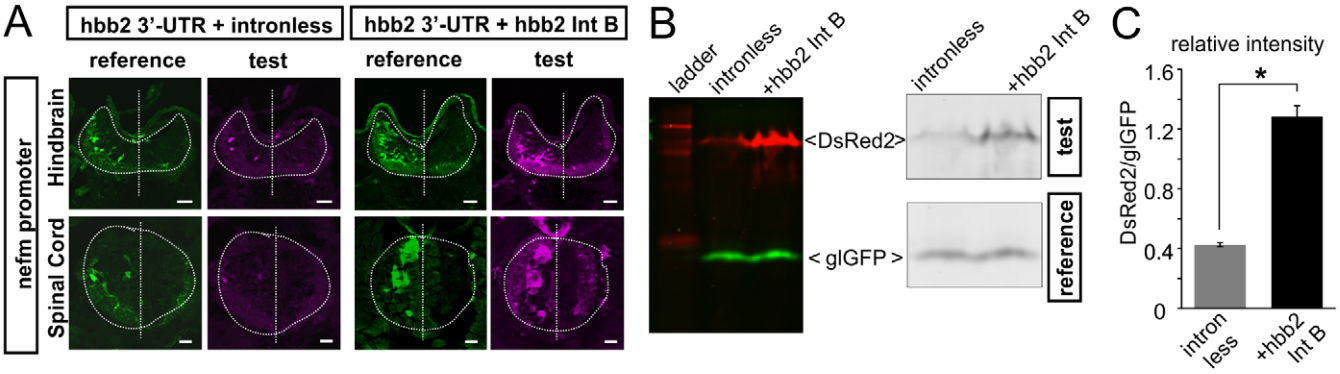

Fig. 6. When driven by the *nefm* promoter and paired with the rabbit β-globin (*hbb2*) 3′-UTR, *hbb2* Intron B also increased reporter protein expression compared with its intronless counterpart. Embryos were co-injected with the same reference plasmid as in Fig. 2 and a test plasmid bearing either no intron (hbb2 3′-UTR+intronless) or the *hbb2* Intron B (hbb2 3′-UTR+hbb2 Int B), all with the *nefm* promoter. Procedures, analyses and annotations were otherwise the same as for Fig. 2. Dotted lines outline the central nervous system. Vertical dotted lines separate the injected and uninjected sides. Scale bars: 20 µm (hindbrain); 50 µm (spinal cord). **P*<0.01 (Student's *t*-test); *n*=3 replicates of 30 pooled embryos for each condition; error bars, s.e.m.

Journal of Cell Science (2016) 129, 1500-1511 doi:10.1242/jcs.185199

(Fig. S1), and compared the effects on protein and RNA expression, as well as on RNA processing and trafficking. We found no significant differences between the two introns in protein expression (Fig. 7A–C), in nascent and total reporter RNA expression (Fig. 7D–F), in nucleocytoplasmic reporter mRNA export (Fig. 7G), or in loading of reporter RNAs onto polysomes for translation (Fig. 7H). Thus, these two introns, originating from two separate genes of different species and having no obvious sequence similarity with one another, were fully interchangeable when coupled with the *nefm* promoter and 3′-UTR.

DISCUSSION

In testing the activity of cis-regulatory elements of the *nefm* gene in live *Xenopus* embryos, we found that incorporating the last intron of *nefm* (Intron II) was essential for achieving optimal reporter protein expression. From analyzing the effects of various intron-bearing and intronless constructs on protein expression, and on the transcription and handling of the RNAs, we conclude that these effects are due to post-transcriptional events requiring both splicing and internal elements of the intron rather than to effects on transcription arising from intronic enhancer elements. The analyses of the handling of the RNAs further demonstrated that differences in protein expression were contingent upon post-transcriptional regulation operating cumulatively at multiple control points, but most chiefly on nucleocytoplasmic export. These conclusions are especially relevant for neurofilament genes because post-transcriptional events underlie many of the changes in neurofilament protein and RNA expression that promote axon development (Moskowitz and Oblinger, 1995; Schwartz et al., 1994) and regeneration (Ananthakrishnan et al., 2008), and also contribute to neurodegenerative diseases (Ge et al., 2003).

Introns have been known since the late 1970s to exert regulatory effects on gene expression (Le Hir et al., 2003). Differences in expression between intron-containing genes and their intronless counterparts have been demonstrated in multiple species, ranging across plants (Bourdon et al., 2001; Callis et al., 1987), invertebrates (Duncker et al., 1997) and vertebrates (Braddock et al., 1994; Buchman and Berg, 1988; Heim et al., 2014; Matsumoto et al., 1998; Palmiter et al., 1991), including mammalian cell lines (Nott et al., 2003). Moreover, these influences can operate on both transcriptional (Brinster et al., 1988; McKenzie and Brennan, 1996; Sleckman et al., 1996) and post-transcriptional control. Post-transcriptional effects extend beyond those associated with nascent RNA splicing to include a full cascade of events associated with RNA metabolism, including polyadenylation, nucleocytoplasmic export, translational efficiency and cytoplasmic decay (Le Hir et al., 2001b; Lewis and Izaurralde, 1997; Liu and Mertz, 1995; Luo and Reed, 1999; Reed and Hurt, 2002; Singh et al., 2012; Vagner et al., 2000). Because these splicing-mediated effects on RNA regulation can differ dramatically among individual intron sequences, their surrounding exon contents, the relative positioning of introns within a gene and the experimental systems in which they are tested, no generic mechanism has been found to account for all varieties of effects (Le Hir et al., 2003; Nott et al., 2003). Hence, each gene must be considered separately, and in the context of the cells and tissues in which it is normally expressed.

Most of the attention paid to the role of introns in the nervous system has been in regard to alternative splicing (de la Grange et al., 2010; Grosso et al., 2008; Zheng and Black, 2013). This layer of regulation contributes considerably to the diversity of neuronal mRNAs and their translated proteins, adding to the dynamic control of neurogenesis, cell migration, and the formation, maturation and function of synapses (Norris and Calarco, 2012). However, because no type IV neurofilament gene is known to undergo alternative splicing, the role intron splicing plays for these genes has up to now gone unstudied. Our study points to a role for introns of neurofilament genes extending beyond alternative splicing to encompass important downstream gene regulatory functions that are crucial for expression.

Results from our experiments with different endogenous and modified introns indicate that, beyond simply having a spliceable intron, what was spliced mattered for subsequent stages of post-transcriptional regulation. Each intronic construct resulted in statistically significant effects on steady-state total RNA levels, but not on nascent RNA transcription, indicative of modest but nonetheless measurable effects on RNA processing. However, far and away the most marked effect was on nucleocytoplasmic export of the mRNAs, which could readily have accounted for the vast differences in protein expression seen among the various *nefm* intron-bearing constructs. These experiments also demonstrated that not only did the two endogenous *nefm* full-length introns vary markedly in their ability to promote (or alternatively, inhibit) nuclear export but also that sequences internal to Intron II were needed because only the full-length but not the minimal spliceable version of this intron led to efficient export. Although the generic importance of intron splicing and the varying abilities of particular introns for promoting nucleocytoplasmic mRNA export have been known for some time (Le Hir et al., 2001b; Luo and Reed, 1999; Reed and Hurt, 2002), our results delineate specific parameters for intron splicing that are most relevant for the *nefm* gene. These parameters differ from those of other genes, such as *oskar*, for which splicing at the position of the first of three exons is required for nuclear export and subsequent localization of the mRNA to the posterior pole of the *Drosophila* embryo, and the third intron can substitute for the first, as long as it is placed into the position of the first intron within the gene (Hachet and Ephrussi, 2004). At this point, we can only speculate whether the observed differences between the two endogenous *nefm* introns might confer any advantages on neurons. One possibility is that splicing of the first intron signals that transcription and processing are as yet incomplete, acting as part of a surveillance mechanism to prevent export and translation of prematurely truncated transcripts (Yap et al., 2015). Translation of such transcripts would be particularly deleterious for NEFM because such truncated transcripts can generate dominant-negative proteins to disrupt pre-existing filaments with severe consequences for the neuron (Lin and Szaro, 1996; Wong and Cleveland, 1990).

Parsing the molecular mechanisms responsible for conferring these optimal properties on the full-length Intron II goes beyond the scope of the current study, for they are undoubtedly complex (Reed, 2003). Possibilities include: (1) influences of exonic sequences adjoining the intron, which were preserved in our constructs and which can sometimes affect deposition of the exon junction complex (Le Hir et al., 2000, 2001b); (2) differences among introns in their associations with trans-factors, which can subsequently be transferred to the spliced mRNA to regulate downstream events (Hachet and Ephrussi, 2001, 2004; Le Hir et al., 2001a, 2003; Lehmann and Nusslein-Volhard, 1986; Micklem et al., 1997; Mohr et al., 2001); and (3) effects of intron length and tertiary structure on splicing efficiency, which can also affect deposition of crucial trans-factors (Ohno et al., 2002). It seems, at least, that length alone cannot be the whole answer because, although the optimally functional *nefm* Intron II (2.9 kb) was notably longer than the non-functional *nefm* Intron I (0.9 kb) and

Journal of Cell Science (2016) 129, 1500-1511 doi:10.1242/jcs.185199

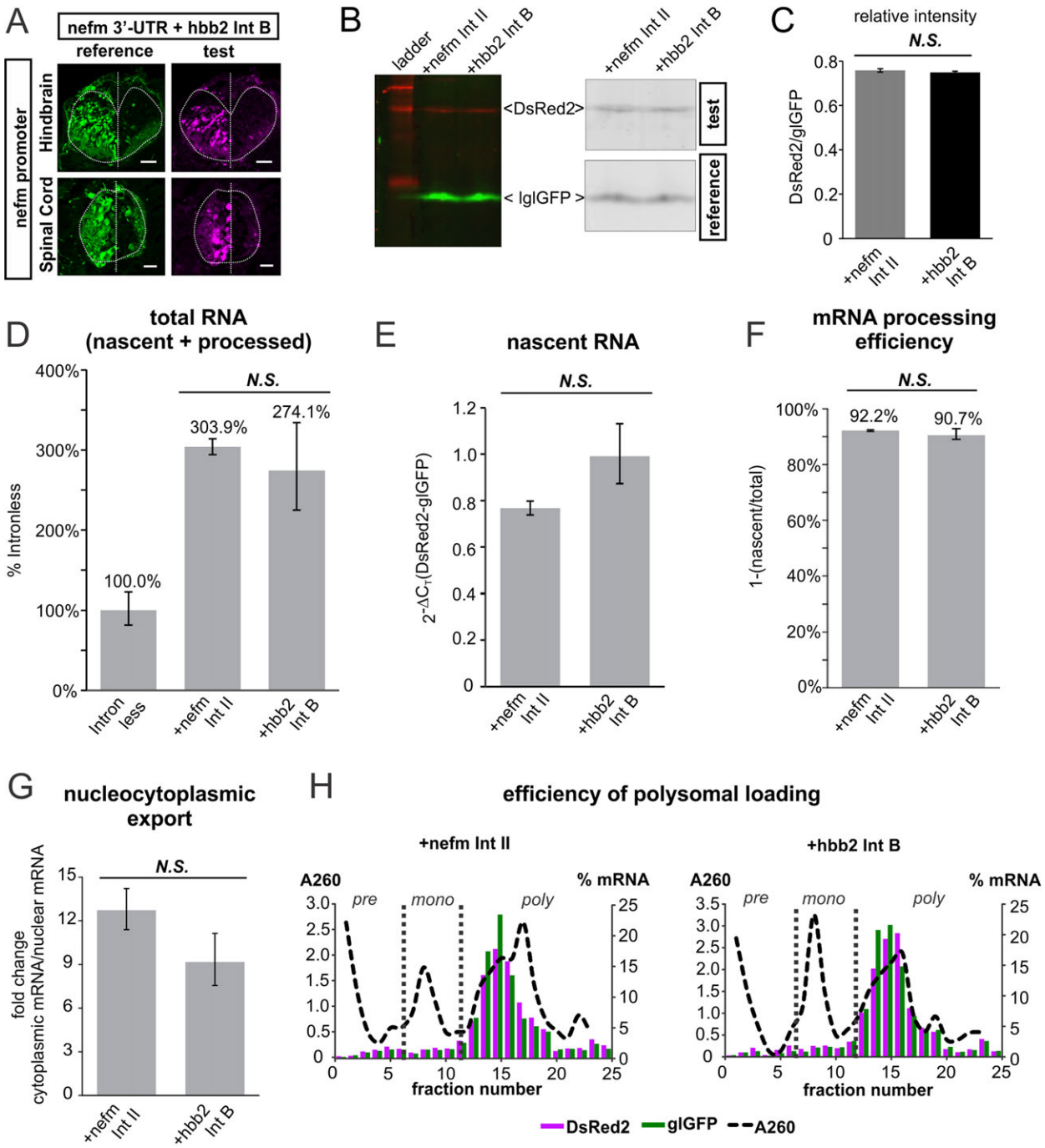

Fig. 7. Post-transcriptional regulation occurred in the same manner for *nefm* Intron II and *hbb2* Intron B when each was paired with the *nefm* 3′-UTR, leading to equivalent amounts of protein expression for both. Embryos were co-injected with the same reference plasmid as described in Fig. 2 and a new test plasmid that contained the *hbb2* Intron B and the *nefm* 3′-UTR. Reporter protein and RNA expression from this construct were then compared with those from the *nefm* Intron II construct. (A–C) The *hbb2* Intron B promoted DsRed2 protein expression at levels comparable to that of *nefm* Intron II. Immunohistochemistry (A, *hbb2 Int B*; Fig. 2, *nefm* Intron II) and quantitative analysis by fluorescent SDS PAGE (B,C) were performed as described in Fig. 2. Dotted lines outline the central nervous system. Vertical dotted lines separate the injected and uninjected sides. Scale bars: 20 µm (hindbrain); 50 µm (spinal cord). (D–H) Analyses of various aspects of RNA regulation showed identical post-transcriptional processing of both RNAs. Analyses in D–G were performed as described in Fig. 4A–D, respectively. (Note, analyses of *gIGFP* reference mRNA processing and nucleocytoplasmic export are shown in Fig. S3, and showed no significant differences across these groups). (H) RNAs arising from both intron groups were also actively loaded onto polysomes for translation to similar extents, as determined from polysomal profiling on sucrose gradients. Left axis: amount of total RNA (dotted line) in each fraction (A_{260}). Fractions occupied by untranslated RNAs (pre), monosomes (mono) and polysomes (poly) are as indicated. Right axis: percentage of *gIGFP* (green bars) and *DsRed2* (magenta bars) reporter RNAs present in the gradient. Error bars are s.e.m.; *n*=3 replicates of 30 pooled embryos (C-F) or *n*=3 biological replicates of ten embryos each (G), for each condition. N.S., *P*>0.05 (Student's *t*-test).

mini spliceable Intron II (0.2 kb), the equally functional *hbb2* Intron B (0.6 kb) was actually slightly shorter than *nefm* Intron I. Thus, differences related to either the tertiary structures of the intron and spliced transcript or the ability of RNA-binding proteins to recognize sequences within the introns seem just as likely to contribute to the effects, if not more so, than intron length alone.

Journal of Cell Science (2016) 129, 1500-1511 doi:10.1242/jcs.185199

At the moment, such properties are difficult to predict solely by using bioinformatics, because of its limited ability to determine folded RNA structures, and because recognition sequences for RNA-binding proteins tend to be short and degenerate (Lagier-Tourenne et al., 2012; Thisted et al., 2001; Tollervey et al., 2011). Hence, the use of an experimental system, such as the one described here using *Xenopus*, will be essential for performing such studies.

In demonstrating the usefulness of *Xenopus* embryos to analyze the contributions of multiple gene regulatory events in the intact organism, our study underscores the importance of intron splicing, extending its role beyond generating mRNA diversity to encompass multiple downstream post-transcriptionally regulated events that culminate in protein expression. Such studies are aimed ultimately at gaining a better understanding of the post-transcriptional regulation of the endogenous *nefm* gene, because such regulation, along with that of the other neurofilament genes, is crucial for axon development and contributes to the pathogenicity of neurodegenerative disorders. We are thus optimistic that this experimental system will provide future insights into the cis-regulatory features and associated trans-factors controlling this regulation *in vivo*. The interchangeable nature of the last introns of two very distinct genes, originating from phylogenetically disparate organisms, further indicates that these properties are both shared among multiple genes and conserved during evolution. Thus, the lessons learned are likely to define a class of mechanisms that applies more broadly to additional genes.

MATERIALS AND METHODS

Preparation of plasmids for microinjection

To obtain promoter-specific reporter expression in F_0 stage 43–44 embryos, we used a modified expression plasmid, which incorporated an *attB* element and two insulators flanking the reporter gene (Wang and Szaro, 2015). For making the *DsRed2* test plasmids used to analyze effects of introns on expression, we first replaced the rabbit β-globin (*hbb2*) 3′-UTR in pSPORT1[*attB*/*Ins1*/(1.5 kb) *NF-M promoter*/*DsRed2*/*β-globin* 3′-UTR/*Ins2*] (Wang and Szaro, 2015) with the *Xenopus nefm* (*NF-M*) 3′-UTR. Introns were then cloned into the *Xho*I site of this construct, which was located within the multiple cloning site of the original *DsRed2* sequences. This site is downstream of the fluorescent protein itself but upstream of the stop codon. Introns were obtained by performing PCR using primers that included nucleotide sequences both upstream of the 5′ and downstream of the 3′ splice sites (5′: 7, 11 and 5 nucleotides; 3′: 20, 17 and 10 nucleotides, for *nefm* Intron II, *nefm* Intron I and *hbb2* Intron B, respectively) to preserve the contexts of the introns. Doing so resulted in a few amino acids (9, 9 and 5, respectively) from the parent protein being retained at the C-terminus of the expressed DsRed2. The mini spliceable Intron II construct retained the 98 and 100 nucleotides from the 5′ and 3′ ends of Intron II, respectively, and the unspliceable Intron II construct lacked 11 and 21 nucleotides from the 5′ and 3′ ends of the intron, respectively. For a complete list of oligonucleotide primers [Integrated DNA Technologies (IDT), Coralville, IA] used to isolate the various elements incorporated into the plasmids and for details on cloning each plasmid, see Table S1. The *nefm* reference plasmid was pSPORT1[*attB*/*Ins1*/(1.5 kb) *NF-M* promoter/*glGFP*/*β-globin* 3′-UTR/*Ins2*], as previously described (Wang and Szaro, 2015). Plasmid DNAs were amplified in Subcloning Efficiency DH5α Competent Cells (Life Technologies), extracted (Wizard Plus Miniprep, Promega; Plasmid Maxi kit, Qiagen) and further purified (Wizard SV Gel and PCR Clean-Up System, Promega) prior to injection.

Microinjection of plasmid DNAs into embryos

All procedures involving animals were approved by the University at Albany's Institutional Animal Care and Use Committee. Fertilized eggs were obtained from breeding pairs of periodic albino (a^p/a^p) *Xenopus laevis* (Hoperskaya, 1975; Tompkins, 1977) through injection of human chorionic gonadotropin (CG-10; Sigma-Aldrich) into the dorsal lymph sac to induce amplexus (Gurdon, 1967). Test and reference plasmid DNAs (75 pg each, in 10 nl) were pressure-co-injected into a single blastomere of two-cell-stage embryos, as described previously (Gervasi and Szaro, 2004). Because in *Xenopus* the descendants of each blastomere in spinal cord, hindbrain and adjacent somites are restricted to one side of the midline (Jacobson and Hirose, 1978), comparing fluorescence between the two sides aided in distinguishing true expression from background autofluorescence, especially for poorly expressing plasmids.

Immunohistochemistry and microscopy

Stage 43–44 tadpoles were anesthetized and fixed, and transverse frozen sections were cut through the hindbrain and spinal cord for immunostaining, as previously described (Wang and Szaro, 2015). The primary antibodies used to detect glGFP and DsRed2 were, respectively: (1) anti-GFP antibody generated in goat (catalog number 600-101-215, lot number 18875, Rockland), 1:500; (2) anti-DsRed antibody generated in rabbit (catalog number 632496, lot number 1306037, Living Colors DsRed polyclonal antibody, Clontech Laboratories), 1:500. Alexa-Fluor-488- (catalog number A11055, lot number 757104, Life Technologies) and Alexa-Fluor-546-conjugated (catalog number A10040, lot number 1218269, Life Technologies) secondary antibodies against the appropriate species were then used (1:1000) to detect the relevant fluorophores. Immunostained sections were imaged by confocal laser scanning microscopy (Zeiss LSM 510 or LSM 710; 20× Plan-ApoChromat; *N.A.*, 0.75; Carl Zeiss AG).

Quantification of reporter protein expression by fluorescent SDS PAGE

To quantify expression of the fluorescent reporter proteins, we adapted a strategy from bacterial studies for visualizing the fluorescent proteins extracted from embryos, directly on partially denaturing SDS 12% polyacrylamide gels (Topilina et al., 2015). For each group, 30 stage 43–44 embryos were homogenized (Polytron 3000, Kinematica AG, Switzerland) in three volumes of lysis buffer [50 mM Tris-HCl, pH 8.0; 10% (vol/vol) glycerol], and the homogenate was spun for 15 min (4°C) in a microcentrifuge (18,400 ***g***) to remove cellular debris. For optimal fluorescence quantification, two-embryo-equivalents of material were then used for each gel. To maintain conditions mild enough to preserve reporter protein fluorescence, the samples were mixed just prior to loading with a loading dye [10% (wt/vol) SDS, 10% (vol/vol) glycerol, 12.5% (vol/vol) stacking buffer, 0.1% bromophenol blue] but without boiling or adding β-mercaptoethanol. Gels were run (Laemmli, 1970) and then imaged for fluorescence immediately afterwards to minimize fluorescence quenching (excitation at 488 nm and 526 nm for glGFP and DsRed2, respectively; Typhoon 9400 scanner, GE Healthcare). All related figures (Figs. 2, 3 and 5–7) show an image of the full gel in color, to visualize coexpression of glGFP and DsRed2 in the same lane (DsRed2 ran as a ∼54 kDa dimer and glGFP as a ∼27 kDa monomer), and separate monochrome images, representative of those used for quantification. The intensity of the DsRed2 band was normalized against that of glGFP in the same lane (NIH ImageJ64), and then averaged (mean±s.e.m.) over three replicate gels for each group. Statistical comparisons across three or more groups were performed using one-way ANOVA, with Tukey's post-hoc tests for identifying significant differences among individual groups. Comparisons between two groups were performed using two-tailed Student's *t*-tests. Differences were considered statistically significant at $P<0.05$. Whether or not differences were significant, power analysis (Faul et al., 2007) was used to confirm that sufficient numbers of samples had been analyzed to support the conclusions (Power>0.8).

Analyses of total RNA expression, nascent RNA expression, mRNA processing, nucleocytoplasmic transport and translation

To maximize recovery of long intron-bearing heterogeneous nuclear (hn) RNAs (Ananthakrishnan et al., 2008), total cellular RNA was obtained from 30 stage 43–44 embryos from each group by performing guanidine-isothiocyanate–CsCl ultracentrifugation (Davis et al., 1994). Resuspended RNA pellets were treated with DNase I (RQ1 RNase-Free DNase, Promega) to further remove any residual DNA contaminant, and the RNA was reverse

transcribed (SuperScript III, Invitrogen) using a mixture of Oligo dT (Invitrogen) and gene-specific primer for *DsRed2* (Table S1), each at 2 pmol.

For analyzing levels of reporter RNA expression (which included both processed mRNAs and nascent unspliced transcript), 5% of the resultant cDNA was subjected to RT-qPCR (7900HT Fast Real-Time PCR System, Life Technologies), using primers from the reporter RNA-coding sequences (Table S1) and SYBR Green PCR Master Mix (Life Technologies). *DsRed2* expression relative to that of *glGFP* (ΔC_T) in the same sample was averaged from three replicates for each group (mean±s.e.m.), and statistical analyses were performed using the same tests and criteria for significance as for analyses of protein expression. For presentation purposes (Figs 4A and 7D), results were first converted to relative expression levels ($2^{-\Delta C_T}$) and then graphed as a percentage of the values for the intronless constructs. To confirm there were no mutations in the resulting spliced RNA generated by the injected embryos, we examined the sequences of the RNA derived from every group by amplifying the above cDNA with primers located in the flanking regions (forward in DsRed2 coding sequence: 5′-GTGATGAA-CTTCGAGGACG-3′; reverse in *nefm* 3′-UTR: 5′-GTAGTATTACAGT-GTCTGGAG-3′), cloning the resultant amplicon into pGEM-T Easy Vector Systems (Promega) by TA-cloning, and sequencing the plasmids extracted from three colonies for each group (GENEWIZ).

For analyzing nascent RNA expression, RT-qPCR was performed in a similar manner on 5% of the same cDNA as described above, but with a forward primer located near to the 3′ end of each intron and a reverse primer from the 5′ end of the downstream 3′-UTR to detect only the unspliced nascent transcript. All primers were designed to generate amplicons of equal length across the groups compared (Table S1). Results for *DsRed2* were normalized against those for *glGFP* present in each sample (ΔC_T), averaged over the samples from the group (mean±s.e.m.), and then converted to a fold-difference ($2^{-\Delta C_T}$; i.e. *DsRed2*/*glGFP*) for presentation. Statistical analyses were performed as described for total RNA expression.

mRNA processing efficiency was calculated by taking the ratio of the amount of nascent reporter RNA to that of total reporter RNA for each sample and subtracting this ratio from 100% [$\Delta C_T = C_{T(\text{nascent RNA})} - C_{T(\text{total RNA})}$; mRNA processing=$100\% - 2^{-\Delta C_T}$]. Samples were averaged and statistical analyses were performed as above. As a control for the quality of the samples, *glGFP* RNA (Figs S2A and S3A) was analyzed separately from *DsRed2* RNA (Figs 4C and 7F) and was appropriately found to be processed in an equivalent manner across all groups.

For measuring nucleocytoplasmic export, subcellular fractionation was performed by homogenizing ten stage 43–44 tadpoles in 500 µl of Polysomal Buffer A (25 mM NaCl, 5 mM $MgCl_2$, 25 mM Tris-HCl pH 7.4; 4°C) containing 10 mM of vanadyl ribonucleoside complex (New England Biolabs) with glass homogenizers and centrifuging the sample at low speed (285 ***g***; 4°C) for 3 min to pellet nuclei (Ananthakrishnan et al., 2008). mRNA was extracted from each fraction (RNeasy Plus kit, Qiagen) and treated as above with DNase I to remove any potentially contaminating DNA. RT-qPCR was then performed to assay reporter RNA expression, as above, with primers targeting reporter coding sequences (Table S1). For each sample, ΔC_T was then determined between cytoplasmic and nuclear RNAs, averaged across biological replicates (n=3 of 10 embryos each), and analyzed for statistical significance as above. The ΔC_T (mean±s.e.m.) was then converted to a fold change ($2^{-\Delta C_T}$) to yield the ratio of the amount of RNA in the cytoplasm/nucleus. As was done for the RNA processing data, *glGFP* RNA (Figs S2B and S3B) was analyzed separately from *DsRed2* RNA (Figs 4D and 7G) and found to be processed equivalently across all groups.

For polysomal profiling, 500 µl of cytoplasmic fraction, prepared as above, was layered onto a 10-ml linear 5–56% (wt/wt) sucrose gradient (Gradient Master 107, BioComp Instruments, Canada) in Polysomal Buffer A and spun in an ultracentrifuge (169,000 ***g***, 4°C, 2 h; SW41 rotor, Beckman Coulter, Pasadena, CA). Fractions (500 µl) were collected (Auto Densi-Flow Density Gradient Fractionator, Labconco, Kansas City, MO, USA), and the macromolecules were precipitated [50 µl 3 M sodium acetate, 20 µl 0.5 M Na_2(EDTA), 2 µl linear acrylamide (Ambion, Life Technologies), 1.5 ml ethanol], resuspended in 200 µl of buffer (0.5% SDS, 0.1 M NaCl, 1 mM EDTA, 10 mM Tris, pH 7.4), and nucleic acids were isolated by performing phenol–chloroform extraction and ethanol precipitation (Davis et al., 1994). The pellets were then resuspended in 50 µl of reaction buffer for DNase I treatment, as above. After an additional round of phenol–chloroform extraction and ethanol precipitation, the final RNA was resuspended in 20 µl water, and 2 µl was used for quantification at A_{260} (NanoDrop ND1000, Thermo Scientific) to distinguish pre-monosomal, monosomal and polysomal fractions. Another 9 µl was used for RT-qPCR with appropriate primers that yielded amplicons of equal length for all RNAs compared (Table S1), and statistical analysis was performed as described for the RNA expression analyses.

Acknowledgements
We thank Enrique Amaya (University of Manchester, UK), Richard Harland (University of California, Berkeley, CA) and Daniel Weeks (University of Iowa, IA) for the *tubb2b* and *actc1* promoters, the *hbb2* 3′-UTR and Intron B, and the original *attB–HS4* plasmids, respectively. We also thank Rupa Priscilla and Christine Gervasi for their help with *Xenopus* spawnings, Min-Ho Lee for providing access to equipment for polysomal profiling and Erica Hutchins for helpful editorial comments.

Competing interests
The authors declare no competing or financial interests.

Author contributions
C.W. conceived, designed and performed the experiments, analyzed and interpreted the data, and wrote the manuscript. B.S. conceived of experiments, interpreted data and wrote the manuscript.

Funding
Financial support for this work came from the National Science Foundation – Division of Integrative Organismal Systems [grant number IOS 1257449 to B.G.S.]; and a pre-doctoral fellowship from the American Association of University Women (International Fellow, C.W.).

Supplementary information
Supplementary information available online at
http://jcs.biologists.org/lookup/suppl/doi:10.1242/jcs.185199/-/DC1

References
Ananthakrishnan, L. and Szaro, B. G. (2009). Transcriptional and translational dynamics of light neurofilament subunit RNAs during *Xenopus laevis* optic nerve regeneration. *Brain Res.* **1250**, 27-40.
Ananthakrishnan, L., Gervasi, C. and Szaro, B. G. (2008). Dynamic regulation of middle neurofilament RNA pools during optic nerve regeneration. *Neuroscience* **153**, 144-153.
Arai, T., Hasegawa, M., Akiyama, H., Ikeda, K., Nonaka, T., Mori, H., Mann, D., Tsuchiya, K., Yoshida, M., Hashizume, Y. et al. (2006). TDP-43 is a component of ubiquitin-positive tau-negative inclusions in frontotemporal lobar degeneration and amyotrophic lateral sclerosis. *Biochem. Biophys. Res. Commun.* **351**, 602-611.
Bennett, G. S., Hollander, B. A. and Laskowska, D. (1988). Expression and phosphorylation of the mid-sized neurofilament protein NF-M during chick spinal cord neurogenesis. *J. Neurosci. Res.* **21**, 376-390.
Bourdon, V., Harvey, A. and Lonsdale, D. M. (2001). Introns and their positions affect the translational activity of mRNA in plant cells. *EMBO Rep.* **2**, 394-398.
Braddock, M., Muckenthaler, M., White, M. R. H., Thorbum, A. M., Sommerville, J., Kingsman, A. J. and Kingsman, S. M. (1994). Intron-less RNA injected into the nucleus of *Xenopus* oocytes accesses a regulated translation control pathway. *Nucleic Acids Res.* **22**, 5255-5264.
Brinster, R. L., Allen, J. M., Behringer, R. R., Gelinas, R. E. and Palmiter, R. D. (1988). Introns increase transcriptional efficiency in transgenic mice. *Proc. Natl. Acad. Sci. USA* **85**, 836-840.
Buchman, A. R. and Berg, P. (1988). Comparison of intron-dependent and intron-independent gene expression. *Mol. Cell. Biol.* **8**, 4395-4405.
Callis, J., Fromm, M. and Walbot, V. (1987). Introns increase gene expression in cultured maize cells. *Genes Dev.* **1**, 1183-1200.
Cañete-Soler, R., Silberg, D. G., Gershon, M. D. and Schlaepfer, W. W. (1999). Mutation in neurofilament transgene implicates RNA processing in the pathogenesis of neurodegenerative disease. *J. Neurosci.* **19**, 1273-1283.
Cao, W., Razanau, A., Feng, D., Lobo, V. G. and Xie, J. (2012). Control of alternative splicing by forskolin through hnRNP K during neuronal differentiation. *Nucleic Acids Res.* **40**, 8059-8071.
Carden, M. J., Trojanowski, J. Q., Schlaepfer, W. W. and Lee, V. M. Y. (1987). Two-stage expression of neurofilament polypeptides during rat neurogenesis with early establishment of adult phosphorylation patterns. *J. Neurosci.* **7**, 3489-3504.

Davis, L. G., Kuehl, W. M. and Battey, J. F. (1994). *Basic Methods in Molecular Biology*. Norwalk: Appleton and Lange.
de la Grange, P., Gratadou, L., Delord, M., Dutertre, M. and Auboeuf, D. (2010). Splicing factor and exon profiling across human tissues. *Nucleic Acids Res.* **38**, 2825-2838.
Duncker, B. P., Davies, P. L. and Walker, V. K. (1997). Introns boost transgene expression in *Drosophila melanogaster*. *Mol. Gen. Genet.* **254**, 291-296.
Faul, F., Erdfelder, E., Lang, A.-G. and Buchner, A. (2007). G*Power 3: a flexible statistical power analysis program for the social, behavioral, and biomedical sciences. *Behav. Res. Methods* **39**, 175-191.
Ge, W.-W., Leystra-Lantz, C., Wen, W. and Strong, M. J. (2003). Selective loss of trans-acting instability determinants of neurofilament mRNA in amyotrophic lateral sclerosis spinal cord. *J. Biol. Chem.* **278**, 26558-26563.
Gervasi, C. and Szaro, B. G. (2004). Performing functional studies of *Xenopus laevis* intermediate filament proteins through injection of macromolecules into early embryos. *Methods Cell Biol.* **78**, 673-701.
Grosso, A. R., Gomes, A. Q., Barbosa-Morais, N. L., Caldeira, S., Thorne, N. P., Grech, G., von Lindern, M. and Carmo-Fonseca, M. (2008). Tissue-specific splicing factor gene expression signatures. *Nucleic Acids Res.* **36**, 4823-4832.
Gurdon, J. B. (1967). African clawed frogs. In *Methods in Developmental Biology* (ed. F. H. Wilt and N. K. Wessels), pp. 75-84. New York: T.Y.Crowell.
Hachet, O. and Ephrussi, A. (2001). *Drosophila* Y14 shuttles to the posterior of the oocyte and is required for *oskar* mRNA transport. *Curr. Biol.* **11**, 1666-1674.
Hachet, O. and Ephrussi, A. (2004). Splicing of *oskar* RNA in the nucleus is coupled to its cytoplasmic localization. *Nature* **428**, 959-963.
Hamer, D. H., Smith, K. D., Boyer, S. H. and Leder, P. (1979). SV40 recombinants carrying rabbit beta-globin gene coding sequences. *Cell* **17**, 725-735.
Heim, A. E., Hartung, O., Rothhamel, S., Ferreira, E., Jenny, A. and Marlow, F. L. (2014). Oocyte polarity requires a Bucky ball-dependent feedback amplification loop. *Development* **141**, 842-854.
Hoperskaya, O. A. (1975). The development of animals homozygous for a mutation causing periodic albinism (a^p) in *Xenopus laevis*. *J. Embryol. Exp. Morphol.* **34**, 253-264.
Jacobson, M. and Hirose, G. (1978). Origin of the retina from both sides of the embryonic brain: a contribution to the problem of crossing at the optic chiasma. *Science* **202**, 637-639.
Kwiatkowski, T. J., Jr., Bosco, D. A., LeClerc, A. L., Tamrazian, E., Vanderburg, C. R., Russ, C., Davis, A., Gilchrist, J., Kasarskis, E. J., Munsat, T. et al. (2009). Mutations in the FUS/TLS gene on chromosome 16 cause familial amyotrophic lateral sclerosis. *Science* **323**, 1205-1208.
Laemmli, U. K. (1970). Cleavage of structural proteins during the assembly of the head of bacteriophage T4. *Nature* **227**, 680-685.
Lagier-Tourenne, C. and Cleveland, D. W. (2009). Rethinking ALS: the FUS about TDP-43. *Cell* **136**, 1001-1004.
Lagier-Tourenne, C., Polymenidou, M., Hutt, K. R., Vu, A. Q., Baughn, M., Huelga, S. C., Clutario, K. M., Ling, S.-C., Liang, T. Y., Mazur, C. et al. (2012). Divergent roles of ALS-linked proteins FUS/TLS and TDP-43 intersect in processing long pre-mRNAs. *Nat. Neurosci.* **15**, 1488-1497.
Le Hir, H., Izaurralde, E., Maquat, L. E. and Moore, M. J. (2000). The spliceosome deposits multiple proteins 20–24 nucleotides upstream of mRNA exon-exon junctions. *EMBO J.* **19**, 6860-6869.
Le Hir, H., Gatfield, D., Braun, I. C., Forler, D. and Izaurralde, E. (2001a). The protein Mago provides a link between splicing and mRNA localization. *EMBO Rep.* **2**, 1119-1124.
Le Hir, H., Gatfield, D., Izauuralde, E. and Moore, M. J. (2001b). The exon-exon junction complex provides a binding platform for factors involved in mRNA export and nonsense-mediated mRNA decay. *EMBO J.* **20**, 4987-4997.
Le Hir, H., Nott, A. and Moore, M. J. (2003). How introns influence and enhance eukaryotic gene expression. *Trends Biochem. Sci.* **28**, 215-220.
Lehmann, R. and Nüsslein-Volhard, C. (1986). Abdominal segmentation, pole cell formation, and embryonic polarity require the localized activity of *oskar*, a maternal gene in *Drosophila*. *Cell* **47**, 141-152.
Lewis, J. D. and Izaurralde, E. (1997). The role of the cap structure in RNA processing and nuclear export. *Eur. J. Biochem.* **247**, 461-469.
Lin, W. and Szaro, B. G. (1996). Effects of intermediate filament disruption on the early development of the peripheral nervous system of *Xenopus laevis*. *Dev. Biol.* **179**, 197-211.
Liu, X. and Mertz, J. E. (1995). HnRNP L binds a *cis*-acting RNA sequence element that enables intron-dependent gene expression. *Genes Dev.* **9**, 1766-1780.
Liu, Y. and Szaro, B. G. (2011). hnRNP K post-transcriptionally co-regulates multiple cytoskeletal genes needed for axonogenesis. *Development* **138**, 3079-3090.
Liu, Y., Gervasi, C. and Szaro, B. G. (2008). A crucial role for hnRNP K in axon development in *Xenopus laevis*. *Development* **135**, 3125-3135.
Luo, M.-J. and Reed, R. (1999). Splicing is required for rapid and efficient mRNA export in metazoans. *Proc. Natl. Acad. Sci. USA* **96**, 14937-14942.
Matsumoto, K., Wassarman, K. M. and Wolffe, A. P. (1998). Nuclear history of a pre-mRNA determines the translational activity of cytoplasmic mRNA. *EMBO J.* **17**, 2107-2121.
McKenzie, R. W. and Brennan, M. D. (1996). The two small introns of the *Drosophila affinidisjuncta Adh* gene are required for normal transcription. *Nucleic Acids Res.* **24**, 3635-3642.
Micklem, D. R., Dasgupta, R., Elliott, H., Gergely, F., Davidson, C., Brand, A., González-Reves, A. and St Johnston, D. (1997). The *mago nashi* gene is required for the polarisation of the oocyte and the formation of perpendicular axes in *Drosophila*. *Curr. Biol.* **7**, 468-478.
Mohr, S. E., Dillon, S. T. and Boswell, R. E. (2001). The RNA-binding protein Tsunagi interacts with Mago Nashi to establish polarity and localize *oskar* mRNA during *Drosophila* oogenesis. *Genes Dev.* **15**, 2886-2899.
Moskowitz, P. F. and Oblinger, M. M. (1995). Transcriptional and post-transcriptional mechanisms regulating neurofilament and tubulin gene expression during normal development of the rat brain. *Mol. Brain Res.* **30**, 211-222.
Moujalled, D., James, J. L., Yang, S., Zhang, K., Duncan, C., Moujalled, D. M., Parker, S. J., Caragounis, A., Lidgerwood, G., Turner, B. J. et al. (2015). Phosphorylation of hnRNP K by cyclin-dependent kinase 2 controls cytosolic accumulation of TDP-43. *Hum. Mol. Genet.* **24**, 1655-1669.
Nie, Z., Wu, J., Zhai, J., Lin, H., Ge, W., Schlaepfer, W. W. and Cañete-Soler, R. (2002). Untranslated element in neurofilament mRNA has neuropathic effect on motor neurons of transgenic mice. *J. Neurosci.* **22**, 7662-7770.
Norris, A. D. and Calarco, J. A. (2012). Emerging roles of alternative pre-mRNA splicing regulation in neuronal development and function. *Front. Neurosci.* **6**, 122.
Nott, A., Meislin, S. H. and Moore, M. J. (2003). A quantitative analysis of intron effects on mammalian gene expression. *RNA* **9**, 607-617.
Ohno, M., Segref, A., Kuersten, S. and Mattaj, I. W. (2002). Identity elements used in export of mRNAs. *Mol. Cell* **9**, 659-671.
Palmiter, R. D., Sandgren, E. P., Avarbock, M. R., Allen, D. D. and Brinster, R. L. (1991). Heterologous introns can enhance expression of transgenes in mice. *Proc. Natl. Acad. Sci. USA* **88**, 478-482.
Rafiq, M., Suen, C. K. M., Choudhury, N., Joannou, C. L., White, K. N. and Evans, R. W. (1997). Expression of recombinant human ceruloplasmin – an absolute requirement for splicing signals in the expression cassette. *FEBS Lett.* **407**, 132-136.
Reed, R. (2003). Coupling transcription, splicing and mRNA export. *Curr. Opin. Cell Biol.* **15**, 326-331.
Reed, R. and Hurt, E. (2002). A conserved mRNA export machinery coupled to pre-mRNA splicing. *Cell* **108**, 523-531.
Roosa, J. R., Gervasi, C. and Szaro, B. G. (2000). Structure, biological activity of the upstream regulatory sequence, and conserved domains of a middle molecular mass neurofilament gene of *Xenopus laevis*. *Mol. Brain Res.* **82**, 35-51.
Schwartz, M. L., Shneidman, P. S., Bruce, J. and Schlaepfer, W. W. (1990). Axonal dependency of the postnatal upregulation in neurofilament expression. *J. Neurosci. Res.* **27**, 193-201.
Schwartz, M. L., Shneidman, P. S., Bruce, J. and Schlaepfer, W. W. (1994). Stabilization of neurofilament transcripts during postnatal development. *Mol. Brain Res.* **27**, 215-220.
Singh, G., Kucukural, A., Cenik, C., Leszyk, J. D., Shaffer, S. A., Weng, Z. and Moore, M. J. (2012). The cellular EJC interactome reveals higher-order mRNP structure and an EJC-SR protein nexus. *Cell* **151**, 750-764.
Sleckman, B. P., Gorman, J. R. and Alt, F. W. (1996). Accessibility control of antigen-receptor variable-region gene assembly: role of *cis*-acting elements. *Annu. Rev. Immunol.* **14**, 459-481.
Strong, M. J., Volkening, K., Hammond, R., Yang, W., Strong, W., Leystra-Lantz, C. and Shoesmith, C. (2007). TDP43 is a human low molecular weight neurofilament (hNFL) mRNA-binding protein. *Mol. Cell. Neurosci.* **35**, 320-327.
Sun, X. and Maquat, L. E. (2000). mRNA surveillance in mammalian cells: the relationship between introns and translation termination. *RNA* **6**, 1-8.
Szaro, B. G. and Gainer, H. (1988). Identities, antigenic determinants, and topographic distributions of neurofilament proteins in the nervous systems of adult frogs and tadpoles of *Xenopus laevis*. *J. Comp. Neurol.* **273**, 344-358.
Szaro, B. G. and Strong, M. J. (2010). Post-transcriptional control of neurofilaments: new roles in development, regeneration and neurodegenerative disease. *Trends Neurosci.* **33**, 27-37.
Szaro, B. G. and Strong, M. J. (2011). Regulation of cytoskeletal composition in neurons: transcriptional and post-transcriptional control in development, regeneration, and disease. *Adv. Neurobiol.* **3**, 559-602.
Szaro, B. G., Lee, V. M.-Y. and Gainer, H. (1989). Spatial and temporal expression of phosphorylated and non-phosphorylated forms of neurofilament proteins in the developing nervous system of *Xenopus laevis*. *Brain Res. Dev. Brain Res.* **48**, 87-103.
Thisted, T., Lyakhov, D. L. and Liebhaber, S. A. (2001). Optimized RNA targets of two closely related triple KH domain proteins, heterogeneous nuclear ribonucleoprotein K and αCP-2KL, suggest distinct modes of RNA recognition. *J. Biol. Chem.* **276**, 17484-17496.

Journal of Cell Science

Thyagarajan, A. and Szaro, B. G. (2004). Phylogenetically conserved binding of specific K Homology domain proteins to the 3′-untranslated region of the vertebrate middle neurofilament mRNA. *J. Biol. Chem.* **279**, 49680-49688.
Thyagarajan, A. and Szaro, B. G. (2008). Dynamic endogenous association of neurofilament mRNAs with K-homology domain ribonucleoproteins in developing cerebral cortex. *Brain Res.* **1189**, 33-42.
Thyagarajan, A., Strong, M. J. and Szaro, B. G. (2007). Post-transcriptional control of neurofilaments in development and disease. *Exp. Cell Res.* **313**, 2088-2097.
Tollervey, J. R., Curk, T., Rogelj, B., Briese, M., Cereda, M., Kayikci, M., König, J., Hortobágyi, T., Nishimura, A. L., Župunski, V. et al. (2011). Characterizing the RNA targets and position-dependent splicing regulation by TDP-43. *Nat. Neurosci.* **14**, 452-458.
Tompkins, R. (1977). Grafting analysis of the periodic albino mutant of *Xenopus laevis*. *Dev. Biol.* **57**, 460-464.
Topilina, N. I., Green, C. M., Jayachandran, P., Kelley, D. S., Stanger, M. J., Piazza, C. L., Nayak, S. and Belfort, M. (2015). SubB intein of *Mycobacterium tuberculosis* as a sensor for oxidative and nitrosative stresses. *Proc. Natl. Acad. Sci. USA* **112**, 10348-10353.
Undamatla, J. and Szaro, B. G. (2001). Differential expression and localization of neuronal intermediate filament proteins within newly developing neurites in dissociated cultures of *Xenopus laevis* embryonic spinal cord. *Cell Motil. Cytoskeleton* **49**, 16-32.
Vagner, S., Vagner, C. and Mattaj, I. W. (2000). The carboxyl terminus of vertebrate poly(A) polymerase interacts with U2AF 65 to couple 3′-end processing and splicing. *Genes Dev.* **14**, 403-413.
Wang, C. and Szaro, B. G. (2015). A method for using direct injection of plasmid DNA to study *cis*-regulatory element activity in F_0 *Xenopus* embryos and tadpoles. *Dev. Biol.* **398**, 11-23.
Wong, P. C. and Cleveland, D. W. (1990). Characterization of dominant and recessive assembly defective mutations in mouse neurofilament NF-M. *J. Cell Biol.* **111**, 1987-2003.
Yap, K., Lim, Z. Q., Khandelia, P., Friedman, B. and Makeyev, E. V. (2015). Coordinated regulation of neuronal mRNA steady-state levels through developmentally controlled intron retention. *Genes Dev.* **26**, 1209-1223.
Zhao, Y. and Szaro, B. G. (1995). The optic tract and tectal ablation influence the composition of neurofilaments in regenerating optic axons of *Xenopus laevis*. *J. Neurosci.* **15**, 4629-4640.
Zheng, S. and Black, D. L. (2013). Alternative pre-mRNA splicing in neurons: growing up and extending its reach. *Trends Genet.* **29**, 442-448.